Linear Motion Control with a Low Power Hydraulic Switching Converter - Part II: Flatness based Control*

Helmut Kogler and Rudolf Scheidl

Institute of Machine Design and Hydraulic Drives
Johannes Kepler University

Altenberger Strasse 69, 4040 Linz, Austria.
helmut.kogler@jku.at, rudolf.scheidl@jku.at
http://imh.jku.at

Abstract

Hydraulic switching control is an opportunity for economic, robust and energy efficient hydraulic motion control. The hydraulic buck converter represents a promising concept, which meets these requirements. Part I of this publication has shown, that for a convenient control performance a model based control should be applied. In this paper a flatness based controller for linear hydraulic motion control with a sub kilowatts hydraulic buck converter is presented. A simple model based on an averaging of the switching converter is employed to derive a flatness based controller combined with a nonlinear observer to estimate all system states only from a position signal. Its performance is studied by simulations and experiments for large ramp type and sinusoidal motions of a heavy mass. Comparison of motion quality and energy consumption are made between the converter and a standard hydraulic proportional drive using a servo-valve instead of the switching converter. With this flatness based controller a tracking performance as good as of a proportional drive can be achieved, yet at much better efficiency. Proportional control for the switching converter, however, leads to inferior results for this type of intended motions.

Keywords: hydraulics, buck converter, flatness based control, switching control

1 Introduction and Retrospection

In electrical engineering switching control is already used for decades, for instance, in switch-mode power supply units. Hydraulic switching control attempts to transfer switching concepts from power electronics to hydraulics in order to make hydraulic drives simpler, cheaper, more robust, and, to raise energy efficiency compared to resistance control. The simplest switching converter concept in hydraulics is the so called hydraulic buck converter (HBC), which is decribed in the following.

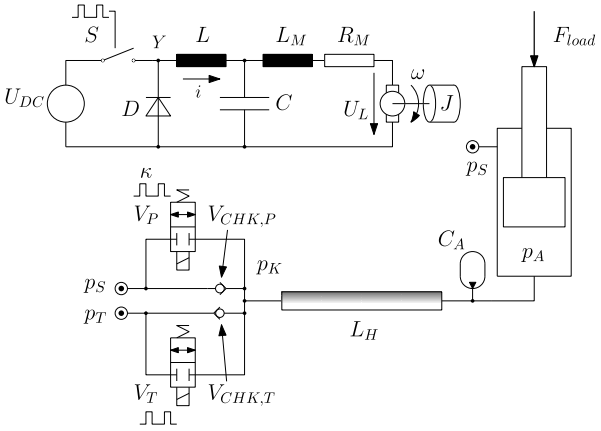

Fig. 1: Electric and hydraulic buck converter schematics

1.1 The Hydraulic Buck Converter

An HBC is the hydraulic pendant to the electric buck converter (EBC). Their basic operating principles are depicted in Fig. 1. In this figure the EBC is used for energy efficient rotary velocity control as presented, for instance, in [1]. Power electronics and DC-motor are considered as one dyamical system, which eases the application advanced control strategies for a performance improvement. In [2, 3] the concept of flatness based control was successfully applied to the EBC-DC-motor configuration, which suggests a corresponding realisation in hydraulics. In contrast to the presented EBC the HBC is used for linear motion control for both mov-

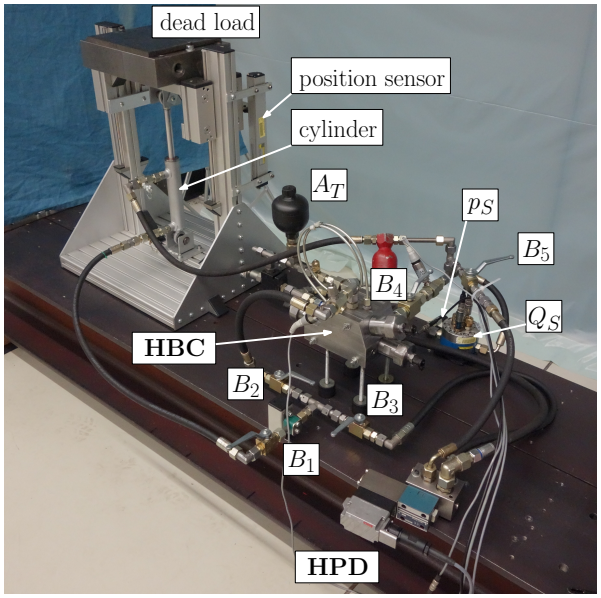

Fig. 2: Test stand

Parameter	Value
dead load	$m = 20\,kg$
diameter of the piston	$d_P = 32\,mm$
diameter of the rod	$d_R = 20\,mm$

Tab. 1: System parameters of the linear drive

ing directions. Only in the extending motion of the hydraulic cylinder the HBC acts in the same way as the EBC, in other words, as an energy efficient step down converter. In the retracting direction the "HBC" actually operates like a boost converter to recuperate energy. Furthermore, in hydraulics the switching frequencies are drastically lower than in power electronics and wave effects in the inductance pipe must be taken into account. Therefore, the design of the HBC and the flatness based approach is different to electrical engineering.

1.2 Linear Motion with a P-Controller

In Part I of the publication the prototype *HBC030* was introduced and the test rig according to Fig. 2 for the intended experiments has been presented. The main dimensions and parameters of the sub kilowatts cylinder drive are listed in Tab. 1. The control performance of the drive was tested by measurements and simulations with a proportional controller according to Fig. 3, which is the simplest closed loop controller for the investigated system. In both cases the design of the controller is carried out empirically. The controller gain was increased until the stability border of the closed loop was crossed, i.e., when the system started to oscillate. The response of the HBC is opposed to a hydraulic proportional drive (HPD). In Fig. 4 the measurements, respectively, the simulation results of the tracking performance with the P-controller are illustrated. The investigations taught, that in fact a lower energy consumption could be proven with the HBC, but the desired control performance could not be achieved with a simple P-controller. This Part II of the publication studies a flatness based controller for the motion control of a system comprising a small HBC driving a hydraulic cylinder which lifts a load. The main motivation to count on this type of control is the severe nonlinearity of the hydraulic accumulator (C_A) which is strongly changing the dynamics of the plant when the pressure p_A varies. The large and varying softness coming from the accumulator allies with the high friction of the small hydraulic cylinder to a nasty control problem.

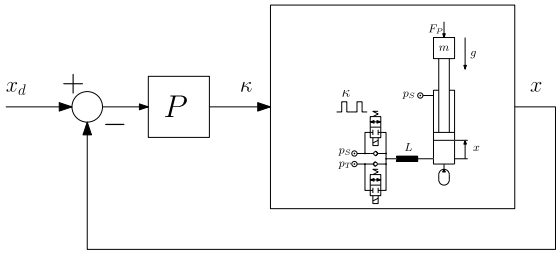

Fig. 3: Control scheme with P-controller

The paper is organized as follows: Chapter 2 deals with the modelling of the HBC for control purposes in order to derive a qualified mathematical model for the controller design. Chapter 3 is devoted to the flatness based controller with a nonlinear observer, which is assessed with an advanced simulation model accounting for effects, which are not considered in the model used for controller design. Chapter 4 shows experimental results obtained with an HBC test rig compared with an HPD. Conclusions and an outlook are given in Chapter 5.

2 Modelling

For a suitable control of the linear drive the pressure fluctuation in the cylinder due to the switching process must be negligibly low. For this reason the accumulator has to be sufficiently large, which makes the load system soft. If the drive is designed properly, the resonator consisting of the dead load m and the gas spring in the accumulator has a natural frequency, which is much lower than the switching frequency of the converter. This frequency gap allows to split up the drive configura-

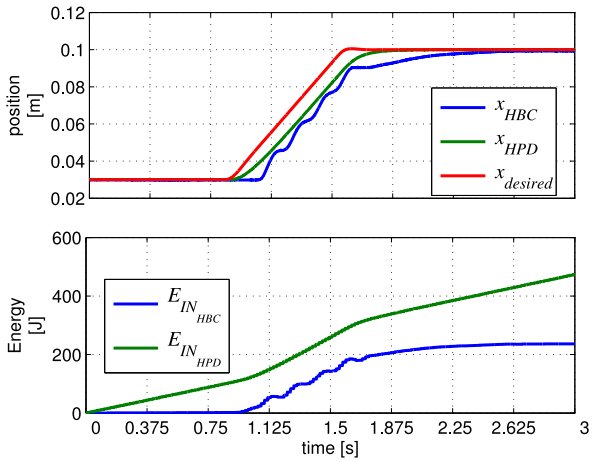

(a) Measurements

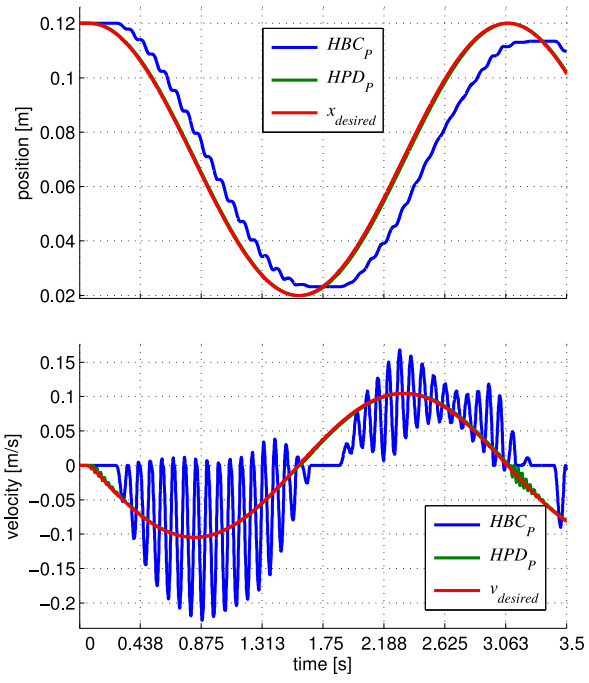

(b) Simulation results

Fig. 4: Trajectory tracking with P-controller

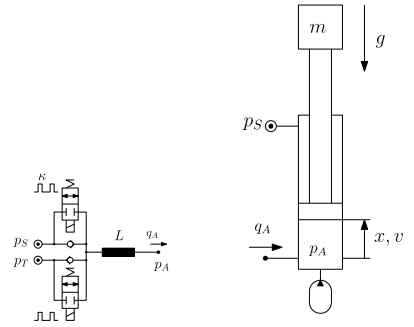

(a) Converter system

(b) Load system

Fig. 5: System segmentation

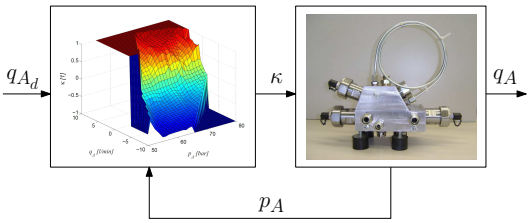

Fig. 6: Inverted converter characteristics

tion into two subsystems with fairly different time constants, as depicted in Fig. 5. Since the partial system of the converter according to Fig. 5a represents a much faster system than the load system, the converter switching can be neglected and the mean value of flow rate q_A in Fig. 5b can be assumed to be constant over one switching cycle. The quasi-static behaviour of the converter can be compensated by its measured steady state characteristics from Fig. 6 for the flatness based control. The diagram shows, for instance, which duty ratio κ is necessary to achieve a flow rate q_A at the output of the converter at a pressure p_A. Thus, the dynamic model for the synthesis of the drive is reduced to the configuration depicted in Fig. 5b. Using the momentum balance of the mechanical part of the system and applying a simple polytropic change of state model for the accumulator results to the following nonlinear autonomous dynamic system

$$\begin{bmatrix} \dot{x} \\ \dot{v} \\ \dot{p}_A \end{bmatrix} = \begin{bmatrix} v \\ \frac{1}{m}\left(p_A A_1 - p_S A_2 - mg - d_v v\right) \\ \frac{p_A \varkappa}{V_A \left(\frac{p_{0_G}}{p_A}\right)^{\frac{1}{\varkappa}}} \left(-A_1 v + q_A\right) \end{bmatrix}, \tag{1}$$

with the state vector

$$\mathbf{x} = \begin{bmatrix} x \\ v \\ p_A \end{bmatrix} \tag{2}$$

and the control input q_A.

3 Flatness Based Control

The control of nonlinear systems along certain trajectories with linear methods results sometimes in a meager performance concerning accuracy. Furthermore, in most cases the stability of the tracking error cannot be proven at all. The gas spring of the pulsation damper at the output of the converter represents a nonlinearity, which cannot be compensated with linear controllers, at least if a linearisation around a steady working point is applied. In the following it will be shown, that the considered differential cylinder driven by an HBC belongs to the special class of flat systems. This property allows a comprehensive dynamic analysis and the design of a powerful controller.

The concept of flatness was introduced by M. Fliess et al. in the 1990ies, see for instance [4]. The basic awareness was the classification of certain nonlinear systems, that behave like linear ones by applying a special type of state feedback. This property of dynamic systems is tightly related to the method of input-output linearisation of nonlinear systems, which can be found, e.g., in Isidori [5]. Another access to flatness is the dynamical invertibility of flat systems. A flat system can be inverted by a feedforward control - depending on the flat output and its derivatives with respect to time - which controls the system along the desired trajectories at least in case of disturbances. For a comprehensive treatment of the flatness concept some knowledge in differential geometry is necessary. But, in this work only the basic definition of flatness and at least some applied mathematical terms are presented in accordance with the literature. To keep the analysis simple, the following considerations focus more on the physical view than on mathematical theory.

The application of the flatness based approach can be separated into three major design steps. First, a feedforward control will be calculated by an exact inversion of the system (1). Hence, in case of no disturbances the output of the system follows the desired trajectory. For this purpose, a flat output y must be found, which allows the intended inversion of the system. Second, the design of a state feedback control is carried out in order to assure that the system follows the desired trajectories in case of disturbances. And third, the state feedback control requires the knowledge of the complete system state. Since only certain state quantities can be measured a state observer must be designed.

The theoretical background for the flatness considerations stems from Rothfuß [6], Rothfuß et al. [7], Rudolph [8]. Further interesting literature concerning flatness is given, for instance, by Lévine [9], Rouchon [10], Sira-Ramírez and Agrawal [11].

3.1 Flat Output and Feedforward Control

The major property of a flat system is that the control input can be described as a function of the so called *flat output* and a finite number of its derivatives with respect to time. With this relation between output and control input, the search of the flat output can be started at the differential equation for the pressure p_A of system (1)

$$\dot{p}_A = \frac{p_A \varkappa}{V_A \left(\frac{p_{0_G}}{p_A}\right)^{\frac{1}{\varkappa}}} \left(-A_1 v + q_A\right), \tag{3}$$

which contains the input q_A. In the following, the individual differential equations of system (1) are considered as a sort of conditional equations. Thus, Eq. (3) represents such an equation for the pressure p_A, which in turn has influence on the mechanical momentum equation

$$m\dot{v} = p_A A_1 - p_S A_2 - mg - d_v v. \tag{4}$$

This equation represents another conditional equation for the velocity v. The momentum equation (4) determines the velocity v, which is conditional for the remaining system equation

$$\dot{x} = v. \tag{5}$$

Since no further conditional development is possible, a flat output is given by

$$y = x. \tag{6}$$

The next step is the calculation of a feedforward control, which must be a function of the flat output and its derivatives with respect to time. Considering system (1) and the chosen output (6) the first and the second derivative with respect to time read

$$\dot{y} = \frac{\partial y}{\partial \mathbf{x}} \dot{\mathbf{x}} = v \tag{7}$$

$$\ddot{y} = \frac{\partial v}{\partial \mathbf{x}} \dot{\mathbf{x}} = \frac{1}{m} \left(p_A A_1 - p_S A_2 - mg - d_v v\right), \tag{8}$$

where all components of the system state $\mathbf{x}$ are present. Using Eqs. (6) to (8) the complete state $\mathbf{x}$ calculates to

$$\begin{bmatrix} x \\ v \\ p_A \end{bmatrix} = \begin{bmatrix} y \\ \dot{y} \\ \frac{1}{A_1}\left(\ddot{y}m + p_S A_2 + mg + d_v \dot{y}\right) \end{bmatrix} = \boldsymbol{\psi}_1\left(y, \dot{y}, \ddot{y}\right) \tag{9}$$

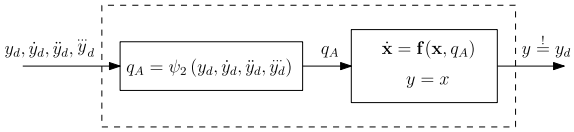

Fig. 7: Inversion of system (1) with the flatness based feedforward control (12)

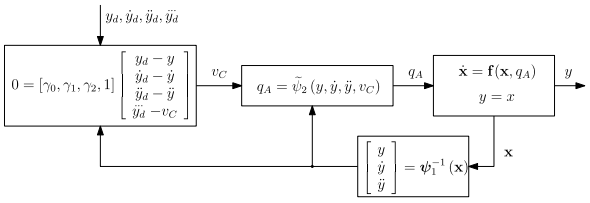

Fig. 8: Flatness based control of system (1)

depending only on the flat output and its derivatives, which is another important property of flat systems. The third derivative of y with respect to time reads

$$\dddot{y} = \frac{\partial \ddot{y}}{\partial \mathbf{x}} \dot{\mathbf{x}} = \frac{1}{m} \left(\dot{p}_A A_1 - d_v \dot{v} \right) \tag{10}$$

$$= \frac{1}{m} \left(\frac{p_A \varkappa A_1 \left(-A_1 v + q_A \right)}{V_A \left(\frac{p_{0_G}}{p_A} \right)^{\frac{1}{\varkappa}}} - \frac{d_v}{m} \left(p_A A_1 - p_S A_2 - mg - d_v v \right) \right), \tag{11}$$

where the input q_A appears. Thus, solving Eq. (11) for q_A leads to the flatness based feedforward control

$$q_A = A_1 \dot{y} + \frac{\left(m \dddot{y} + d_v \ddot{y} \right) V_A \left(\frac{p_{0_G} A_1}{p_S A_2 + d_v \dot{y} + m \ddot{y} + mg} \right)^{\frac{1}{\varkappa}}}{\varkappa \left(p_S A_2 + d_v \dot{y} + m \ddot{y} + mg \right)}$$

$$= \psi_2 \left(y, \dot{y}, \ddot{y}, \dddot{y} \right). \tag{12}$$

With the conditions of Eq. (6), Eq. (9) and Eq. (12) it could be shown, that the considered system (1) is flat.

The feedforward control (12) provides an exact inversion of system (1), like depicted in Fig. 7, at least if no disturbances influence the system.

3.2 Controller Design

The flat output and its derivatives from Eqs. (6) to (8) can be written as

$$\begin{bmatrix} y \\ \dot{y} \\ \ddot{y} \end{bmatrix} = \begin{bmatrix} x \\ v \\ \frac{1}{m} \left(p_A A_1 - p_S A_2 - mg - d_v v \right) \end{bmatrix} = \boldsymbol{\psi}_1^{-1}(\mathbf{x}). \tag{13}$$

This means, that if the state $\mathbf{x}$ is known, the actual flat output y and its derivatives with respect to time are known too. Thus, Eq. (13) can be used for a static state feedback. For this purpose, the transformed state (13) is applied to Eq. (12), which results in a state feedback

$$q_A = \widetilde{\psi}_2 \left(\mathbf{x}, v_C \right) \tag{14}$$

with a new input v_C, which is related to the third derivative of the flat output with respect to time. Furthermore, the trajectory error is defined by

$$\begin{bmatrix} e \\ \dot{e} \\ \ddot{e} \\ \dddot{e} \end{bmatrix} = \begin{bmatrix} y_d - y \\ \dot{y}_d - \dot{y} \\ \ddot{y}_d - \ddot{y} \\ \dddot{y}_d - v_C \end{bmatrix} \tag{15}$$

with the input v_C of the state feedback (14) and the desired trajectory y_d. Hence, with $y = x$ the dynamics of the position error $e = y_d - x$ can be written as

$$0 = \begin{bmatrix} \gamma_0 & \gamma_1 & \gamma_2 & 1 \end{bmatrix} \begin{bmatrix} y_d - y \\ \dot{y}_d - \dot{y} \\ \ddot{y}_d - \ddot{y} \\ \dddot{y}_d - v_C \end{bmatrix}$$

$$= \dddot{y}_d - v_C + \gamma_2 \ddot{e} + \gamma_1 \dot{e} + \gamma_0 e, \tag{16}$$

which represents a linear differential equation. Extracting v_C from Eq. (16) the resulting control law reads

$$v_C = \dddot{y}_d + \gamma_2 \ddot{e} + \gamma_1 \dot{e} + \gamma_0 e \tag{17}$$

with the parameters γ_i, $i = 0, 1, 2$. The block diagram of this flatness based control is depicted in Fig. 8. To assure asymptotic stability of the trajectory error all poles of Eq. (16) must have negative real parts. This is related to the roots of the cubical characteristic polynomial

$$s^3 + \gamma_2 s^2 + \gamma_1 s + \gamma_0 = 0. \tag{18}$$

Since the flat output $y = x$ represents a position, its third derivative $\dddot{y}$ has the unit $\frac{m}{s^3}$. Thus, the units of γ_0, γ_1 and γ_2 read $\frac{1}{s^3}$, $\frac{1}{s^2}$ and $\frac{1}{s}$, respectively, and the choice of the poles for the closed loop system allows a physical interpretation as a PDDD-controller for the position of the linear hydraulic drive.

3.3 Observer Design

The static state feedback (13) requires the knowledge of the complete state $\mathbf{x}$ of system (1). But in common industrial applications no measurement of the piston velocity is provided. Furthermore, for

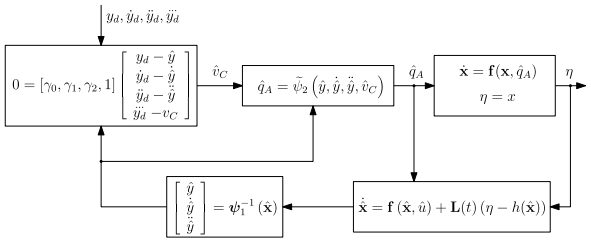

Fig. 9: Block diagram of the intended control exploiting a nonlinear observer

cost reasons it is better to avoid a sensor for the pressure p_A. Hence, the whole system state cannot be measured and, thus, a dynamic state observer has to be designed. The following considerations are carried out in accordance with Fliess and Rudolph [12] and Rothfuß et al. [7].

For the investigated nonlinear system (1) an observer of the form

$$\dot{\hat{\mathbf{x}}} = \mathbf{f}(\hat{\mathbf{x}}, \hat{u}) + \mathbf{L}(t)(\eta - h(\hat{\mathbf{x}})), \ \hat{\mathbf{x}}(0) = \hat{\mathbf{x}}_0 \quad (19)$$

with the estimated state $\hat{\mathbf{x}}$, the generally time varying observer gain $\mathbf{L}(t)$, and the measured quantity η, is intended. Under the assumption that the flatness based control keeps the system state sufficiently close to the desired trajectories, $\hat{u} = \hat{q}_A$ represents the input of the closed loop system. The intended flatness based control with a nonlinear observer is depicted in Fig. 9.

The dynamics of the estimation error $\hat{\mathbf{e}} = \hat{\mathbf{x}} - \mathbf{x}$ reads

$$\dot{\hat{\mathbf{e}}} = \mathbf{f}(\hat{\mathbf{x}}, \hat{u}) - \mathbf{f}(\mathbf{x}, \hat{u}) + \mathbf{L}(t)(h(\mathbf{x}) - h(\hat{\mathbf{x}})), \quad (20)$$

which represents a system of nonlinear differential equations. For a convenient analysis Eq. (20) must be linearised. Since the hydraulic drive is designed to move certain loads a linearisation around a steady working point is not sufficient. Thus, the nonlinear estimation error system (20) can be linearised around the desired trajectories under the assumption that the control keeps the system state sufficiently close to the desired trajectories. This assumption leads to a linear time varying design problem. The linearisation of Eq. (20) along the desired trajectory calculates to

$$\dot{\hat{\mathbf{e}}} = \underbrace{\left[\mathbf{A}(t)\,\widehat{\Delta\mathbf{x}} + \mathbf{b}(t)\,\Delta u + \mathbf{L}(t)\left(\mathbf{c}^\top \Delta\mathbf{x} - \mathbf{c}^\top \widehat{\Delta\mathbf{x}}\right)\right]}_{\text{observer}} - \underbrace{\left[\mathbf{A}(t)\,\Delta\mathbf{x} + \mathbf{b}(t)\,\Delta u\right]}_{\text{system}} \quad (21)$$

with

$$\mathbf{A}(t) = \left.\frac{\partial}{\partial \mathbf{x}}\mathbf{f}(\mathbf{x}, u)\right|_{\mathbf{x}_d(t), u_d(t)}, \quad (22)$$

$$\mathbf{b}(t) = \left.\frac{\partial}{\partial u}\mathbf{f}(\mathbf{x}, u)\right|_{\mathbf{x}_d(t), u_d(t)}, \quad (23)$$

$$\mathbf{c}^\top = \left.\frac{\partial}{\partial \mathbf{x}}h(\mathbf{x})\right|_{\mathbf{x}_d(t), u_d(t)} \quad (24)$$

and the output equation $y = h(\mathbf{x})$ of the original nonlinear system. Substituting $\widehat{\Delta\mathbf{x}} = \hat{\mathbf{x}} - \mathbf{x}_d$, $\Delta\mathbf{x} = \mathbf{x} - \mathbf{x}_d$, $\hat{\mathbf{e}} = \hat{\mathbf{x}} - \mathbf{x}$ and $\Delta u = \hat{u} - u_d$ into Eq. (21) the linearised observer dynamics of Eq. (20) follows to

$$\dot{\hat{\mathbf{e}}} = \left(\mathbf{A}(t) - \mathbf{L}(t)\mathbf{c}^\top\right)\hat{\mathbf{e}}. \quad (25)$$

The time varying observer gain $\mathbf{L}(t)$ in Eq. (25) has to be designed for asymptotic stability of the estimation error $\hat{\mathbf{e}}$. But, before the observer can be designed, the observability of the linearised system

$$\Delta\dot{\mathbf{x}} = \mathbf{A}(t)\Delta\mathbf{x} + \mathbf{b}(t)\Delta u \quad (26)$$

$$\Delta\eta = \mathbf{c}^\top \Delta\mathbf{x} \quad (27)$$

must be checked. Therefore it is necessary, that components of the state can be calculated from the output $\Delta\eta$ and its derivatives with respect to time. This is only possible if the following expressions

$$\Delta\eta = \mathbf{c}^\top \Delta\mathbf{x} \quad (28)$$

$$\Delta\dot{\eta} = \left[\frac{\mathrm{d}}{\mathrm{d}t}\mathbf{c}^\top + \mathbf{c}^\top \mathbf{A}(t)\right]\Delta\mathbf{x} = \left[\left(\mathbf{A}^\top(t) + \frac{\mathrm{d}}{\mathrm{d}t}\right)\mathbf{c}\right]^\top \Delta\mathbf{x} \quad (29)$$

$$\Delta\ddot{\eta} = \frac{\mathrm{d}}{\mathrm{d}t}\left[\frac{\mathrm{d}}{\mathrm{d}t}\mathbf{c}^\top + \mathbf{c}^\top \mathbf{A}(t)\right]\Delta\mathbf{x} + \left[\frac{\mathrm{d}}{\mathrm{d}t}\mathbf{c}^\top + \mathbf{c}^\top \mathbf{A}(t)\right]\mathbf{A}(t)\Delta\mathbf{x} = \left[\left(\mathbf{A}^\top(t) + \frac{\mathrm{d}}{\mathrm{d}t}\right)^2 \mathbf{c}\right]^\top \Delta\mathbf{x}, \quad (30)$$

can be calculated, i.e. the observability matrix

$$\mathbf{Q}(t) = \begin{bmatrix} \mathbf{c}^\top \\ M_{\mathbf{A}(t)}\mathbf{c}^\top \\ M^2_{\mathbf{A}(t)}\mathbf{c}^\top \end{bmatrix} \quad (31)$$

has full rank, where $M_{\mathbf{A}(t)}$ represents the differential operator

$$M_{\mathbf{A}(t)}\mathbf{t}_1^\top = \mathbf{t}_1^\top \mathbf{A}(t) + \dot{\mathbf{t}}_1^\top \quad (32)$$

$$M^{k+1}_{\mathbf{A}(t)}\mathbf{t}_1^\top = M_{\mathbf{A}(t)}\left(M^k_{\mathbf{A}(t)}\mathbf{t}_1^\top\right), \ k > 0 \quad (33)$$

$$M^0_{\mathbf{A}(t)}\mathbf{t}_1^\top = \mathbf{t}_1^\top \quad (34)$$

for time dependent[1] row vectors $\mathbf{t}_1^\intercal$ and the matrix $\mathbf{A}(t)$. But, even if system (26) is observable negative real parts of the eigenvalues of the error dynamics (25) do not guarantee stability, since it is a time varying system. In order to assure the stability of the estimation error the time variance must be compensated, which can be done in the observer's canonical form. The necessary change of coordinates reads

$$\boldsymbol{\zeta} = \boldsymbol{\Theta}(t)\mathbf{x}, \tag{35}$$

which is a regular transformation. In Eq. (35) the vector $\boldsymbol{\zeta}$ represents the state in coordinates of the canonical form. The calculation of $\boldsymbol{\Theta}(t)$ requires the differential operator $N_{\mathbf{A}(t)}$

$$\begin{aligned} N_{\mathbf{A}(t)}\mathbf{b} &= \mathbf{A}(t)\mathbf{b} - \dot{\mathbf{b}} && (36)\\ N^{k+1}_{\mathbf{A}(t)}\mathbf{b} &= N_{\mathbf{A}(t)}\left(N^{k}_{\mathbf{A}(t)}\mathbf{b}\right),\ k>0 && (37)\\ N^{0}_{\mathbf{A}(t)}\mathbf{b} &= \mathbf{b} && (38) \end{aligned}$$

for column vectors $\mathbf{b}$ applied to the matrix $\mathbf{A}(t)$.

In the concrete case the design of a complete observer will be presented. The resulting performance of the different observer designs will be verified by simulations in *Matlab/Simulink*$^{\mathrm{TM}}$.

The complete observer type estimates the full system state, even though only one state variable

$$\eta = h(\mathbf{x}) = x, \tag{39}$$

the position of the dead load, is measured. As pointed out before, the linearisation of system (1) along the trajectory leads to a linear time varying dynamical system with

$$\begin{aligned} \mathbf{A}(t) &= \begin{bmatrix} 0 & 1 & 0 \\ 0 & -\frac{d_v}{m} & \frac{A_1}{m} \\ 0 & -\frac{A_1 \varkappa p_A(t)}{V_A\left(\frac{p_{0G}}{p_A(t)}\right)^{\frac{1}{\varkappa}}} & \frac{(-A_1 v(t)+q_A(t))(\varkappa+1)}{V_A\left(\frac{p_{0G}}{p_A(t)}\right)^{\frac{1}{\varkappa}}} \end{bmatrix}\\ \mathbf{c}^\top &= \begin{bmatrix} 1 & 0 & 0 \end{bmatrix}. \end{aligned}$$

For a better readability, the entries of the matrix $\mathbf{A}(t)$ are abbreviated according to

$$\mathbf{A}(t) = \begin{bmatrix} 0 & 1 & 0 \\ 0 & a_{22} & a_{23} \\ 0 & a_{32}(t) & a_{33}(t) \end{bmatrix}. \tag{40}$$

Before the observer is designed, the observability is checked by the calculation of the observability matrix

$$\begin{aligned} \mathbf{Q} &= \begin{bmatrix} \mathbf{c}^\top \\ M_{\mathbf{A}(t)}\mathbf{c}^\top \\ M^2_{\mathbf{A}(t)}\mathbf{c}^\top \end{bmatrix}\\ &= \begin{bmatrix} 1 & 0 & 0 \\ 0 & 1 & 0 \\ 0 & a_{22} & a_{23} \end{bmatrix}. \end{aligned} \tag{41}$$

[1] For better readability the argument t of the time dependent vectors $\mathbf{t}_1^\intercal$ is omitted.

This matrix has full rank for every point in time and, thus, the linearised system is observable. The time varying state transformation to the canonical form calculates to

$$\begin{aligned} \boldsymbol{\Theta}^{-1}(t) &= \begin{bmatrix} \boldsymbol{\theta} & N_{\mathbf{A}(t)}\boldsymbol{\theta} & N^2_{\mathbf{A}(t)}\boldsymbol{\theta} \end{bmatrix}\\ &= \begin{bmatrix} 0 & 0 & 1 \\ 0 & 1 & a_{22}+a_{33}(t) \\ \frac{1}{a_{23}} & \frac{a_{33}(t)}{a_{23}} & a_{32(t)} + \frac{a^2_{33}(t)}{a_{23}} + \frac{\frac{\mathrm{d}}{\mathrm{d}t}a_{33}(t)}{a_{23}} \end{bmatrix} \end{aligned} \tag{42}$$

with

$$\boldsymbol{\theta} = \mathbf{Q}^{-1}\begin{bmatrix} 0 \\ 0 \\ 1 \end{bmatrix} \tag{43}$$

and $N_{\mathbf{A}(t)}$ according to Eq. (36). With Eq. (42) the desired canonical form follows to

$$\begin{aligned} \mathbf{A}^\star(t) &= \left(\frac{\mathrm{d}}{\mathrm{d}t}\boldsymbol{\Theta}(t) + \boldsymbol{\Theta}(t)\mathbf{A}(t)\right)\boldsymbol{\Theta}^{-1}(t)\\ &= \begin{bmatrix} 0 & 0 & a_{22}\frac{\mathrm{d}}{\mathrm{d}t}a_{33}(t) + \frac{\mathrm{d}^2}{\mathrm{d}t^2}a_{33}(t) - a_{23}\frac{\mathrm{d}}{\mathrm{d}t}a_{32}(t) \\ 1 & 0 & a_{23}a_{32}(t) - a_{33}(t)a_{22} - 2\frac{\mathrm{d}}{\mathrm{d}t}a_{33}(t) \\ 0 & 1 & a_{32}(t) + a_{33}(t) \end{bmatrix}. \end{aligned} \tag{44}$$

The time varying entries of matrix (44) can be compensated in this canonical form by the design vector

$$\mathbf{L}^\star(t) = \begin{bmatrix} \alpha_0 + a_{22}\frac{\mathrm{d}}{\mathrm{d}t}a_{33}(t) + \frac{\mathrm{d}^2}{\mathrm{d}t^2}a_{33}(t) - a_{23}\frac{\mathrm{d}}{\mathrm{d}t}a_{32}(t) \\ \alpha_1 + a_{23}a_{32(t)} - a_{33}(t)a_{22} - 2\frac{\mathrm{d}}{\mathrm{d}t}a_{33}(t) \\ +\alpha_2 + a_{32}(t) + a_{33}(t) \end{bmatrix}, \tag{45}$$

which leads to the dynamic matrix of the state observer

$$\mathbf{A}^\star(t) - \mathbf{L}^\star(t)\begin{bmatrix} 0 & 0 & 1 \end{bmatrix} = \begin{bmatrix} 0 & 0 & -\alpha_0 \\ 1 & 0 & -\alpha_1 \\ 0 & 1 & -\alpha_2 \end{bmatrix} \tag{46}$$

with the characteristic polynomial of the observation error

$$s^3 + \alpha_2 s^2 + \alpha_1 s + \alpha_0 = 0, \tag{47}$$

which must be a Hurwitz-Polynomial[2] in s. The observer parameters $\alpha_i,\ i = 0, 1, 2$ must be adjusted properly for asymptotic stability.

In original coordinates the flatness based complete

[2] All roots of a Hurwitz-Polynomial have negative real parts.

observer reads

$$\dot{\hat{\mathbf{x}}} = \mathbf{f}(\hat{\mathbf{x}},\hat{u}) + \mathbf{\Theta}^{-1}(t)\mathbf{L}^{\star}(t)(\eta - h(\hat{\mathbf{x}})) \quad (48)$$

$$= \begin{bmatrix} \hat{v} \\ \frac{1}{m}\left(\hat{p}_A A_1 - p_S A_2 - mg - d_v\hat{v}\right) \\ \frac{\hat{p}_A \varkappa}{V_A\left(\frac{p_{0_G}}{\hat{p}_A}\right)^{\frac{1}{\varkappa}}}\left(-A_1\hat{v} + \hat{q}_A\right) \end{bmatrix}$$

$$+ \left(\begin{bmatrix} \left(\alpha_2 - \frac{d_v}{m} + \vartheta(t)\right) \\ \left(\alpha_1 - 2\frac{\mathrm{d}\vartheta(t)}{\mathrm{d}t} - \frac{d_v\vartheta(t) + \varsigma(t)A_1 - d_v\alpha_2 + d_v^2}{m}\right) \\ \Upsilon(t) \end{bmatrix} \right.$$

$$\left. + \begin{bmatrix} 0 \\ \left(\vartheta(t)\alpha_2 + \vartheta^2(t)\right) \\ 0 \end{bmatrix} \right) (x - \hat{x}) \quad (49)$$

with

$$\Upsilon(t) = \frac{m\alpha_0}{A_1} - \frac{\mathrm{d}\varsigma(t)}{\mathrm{d}t} + \frac{m\frac{\mathrm{d}^2\vartheta(t)}{\mathrm{d}t^2} + \vartheta(t)m\alpha_1 - 3\vartheta(t)m\frac{\mathrm{d}\vartheta(t)}{\mathrm{d}t}}{A_1} + 2\vartheta(t)\varsigma(t) + \alpha_2\varsigma(t) - \frac{\varsigma(t)d_v}{m} + \frac{\vartheta(t)^2 m\alpha_2 + \vartheta(t)^3 m - \frac{\mathrm{d}\vartheta(t)}{\mathrm{d}t}\alpha_2 m}{A_1}, \quad (50)$$

$$\varsigma(t) = -\frac{A_1 p_{A_d}\varkappa}{V_A\left(\frac{p_{0_G}}{p_{A_d}}\right)^{\frac{1}{\varkappa}}}, \quad (51)$$

$$\vartheta(t) = -\frac{(\varkappa+1)\left(A_1 v_d - q_{A_d}\right)}{V_A\left(\frac{p_{0_G}}{p_{A_d}}\right)^{\frac{1}{\varkappa}}}, \quad (52)$$

where $\eta = x$ denotes the measured position of the dead load and $\hat{\mathbf{x}} = [\hat{x}\ \hat{v}\ \hat{p}_A]^\top$ represents the state of the observer. It is important to mention, that the observer (48) requires the knowledge of the desired trajectories $\mathbf{x}_d$ and u_d. Since in the concrete case the flatness based control is a sort of a PDDD-controller, the desired trajectory of the flat output and, further, a number of its derivatives with respect to time have to be provided. Furthermore, this flatness based observer requires the fourth and fifth derivative of the desired flat output according to Eq. (50), which puts corresponding continuity requirements on the desired trajectories generation. This can be realised either offline by pre-processing or by the implementation of a pre-filter as shown in the following section.

3.4 Trajectory Planning

As pointed out in the previous subsections the desired trajectory and a finite number of its derivatives with respect to time must be provided for the flatness based controller. Basically, there are two possibilities to fulfill this requirement. First, the trajectory can be planned by pre-processing in offline mode. Therefore, the intended motion of the system must be known and parameterised before the application goes into operation. In many cases the desired trajectory is uncertain itself, moreover it is governed by the operator of the drive during the working process. In such cases a second method is applicable. It uses a certain pre-filter, which delivers a trajectory with all its derivatives necessary for the controller. Since such a filter represents a sort of differentiator, this method only works in a certain dynamic operating range. There exist a number of methods to calculate the necessary derivatives for a flatness based control in online mode, as for instance in von Löwis and Rudolph [13]. However, in this work a digital pre-filter according to Wolfram and Vogt [14] is used.

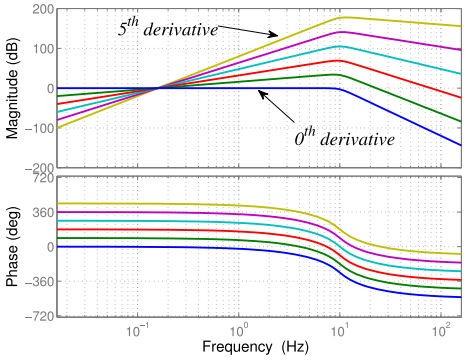

Fig. 10: Bode plots of the filter according to Eq. (54) for differentiation of order 0 (just amplification) up to order 5

Basically, a transfer function of the form

$$G(s) = \frac{1}{\tau_\sigma s^\sigma + \ldots + \tau_1 s + 1}, \quad (53)$$

with σ as the number of necessary derivatives, is qualified for online trajectory planning. Such a filter can be, for instance, a *Bessel-*, *Butterworth* or any other low pass filter of sufficient order. The continuous transfer function (53) is equivalent to the canonical form in state space

$$\begin{aligned} \dot{\mathbf{x}} &= \mathbf{A}_C\mathbf{x} + \mathbf{b}_C u \\ \mathbf{y} &= \mathbf{C}_C\mathbf{x} + \mathbf{d}_C u. \end{aligned} \quad (54)$$

In this canonical form the entries of the state $\mathbf{x}$ correspond to the derivatives of the filtered signal u. The filter, which is parameterised for the flatness based control of the linear hydraulic drive powered by the HBC, is illustrated in Fig. 10. Since an ideal differentiator is not realisable, the filter has a cut-off frequency. In this case the maximum frequency

of the desired operating cycles is limited to approximately $10\,Hz$. For implementation on a digital signal processing unit the continuous filter of Eq. (54) must be discretised with a constant sample time T_S.

3.5 Simulation

The block diagram of the flatness based control (FBC) employing a complete observer is illustrated in Fig. 11, where the advantage of this observer type becomes clear. The nonlinear observer estimates the whole system state $\hat{\mathbf{x}} = [\hat{x}\ \hat{v}\ \hat{p}_A]^\top$, which is necessary for the FBC, just by measuring the position of the load x. The set variable of the nonlinear controller is the flow rate q_A, which must be transformed to a duty ratio κ by the inversed static converter characteristic according to Fig. 6.

The first simulation case considers a ramp in both moving directions with a constant slope of $v_d = 100\frac{mm}{s}$. The corresponding results are illustrated in Fig. 12, where the flatness based control is compared to a conventional hydraulic proportional drive.

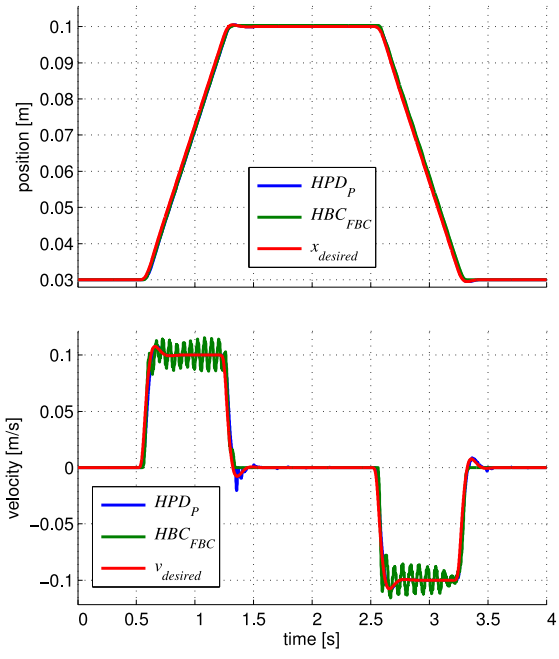

Fig. 12: Simulated trajectory tracking of the FBC

In Fig. 13 simulation results of a $0.2\,Hz$ sinusoidal trajectory are presented.

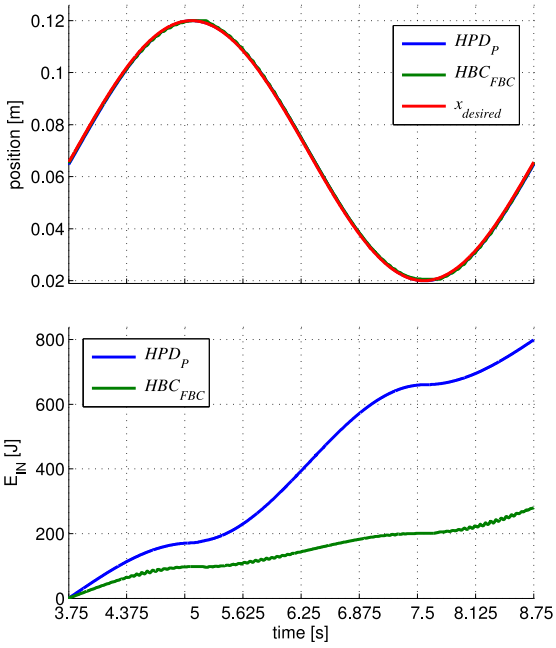

Fig. 13: Energy consumption of the FBC at trajectory tracking simulations

In the lower diagram the energy consumptions of both drive concepts are depicted. The HBC in combination with an FBC needs for a similar performance less than half of the power of the HPD in this specific case. It must be remarked, that the overall drive configuration represents a nonlinear system, which prevents an extrapolation of the illustrated results to other power dimensions. Also the specific load scenarios play a significant role for the energy consumption of such drives.

4 Measurements

In the following, results of the experiments on the closed loop performance of the HBC are compared with a conventional proportional drive (HPD) with the test rig according to Fig. 2. The flatness based control is realised according to Fig. 11 on a *dSpace DS1103 PPC Controller Board*. The characteristic diagram from Fig. 6 is used to compensate the static characteristics of the switching converter. The dynamics of the nonlinear flatness based observer is implemented quasi-continuously, which means, that the nonlinear differential equations are approximated by an Adams-Bashforth-Algorithm with a much higher sampling frequency than the time constants of the observer dynamics. The flatness based control is represented by algebraic equations, since the dynamics of the system is parameterised by the planned trajectories according to the filter design described above.

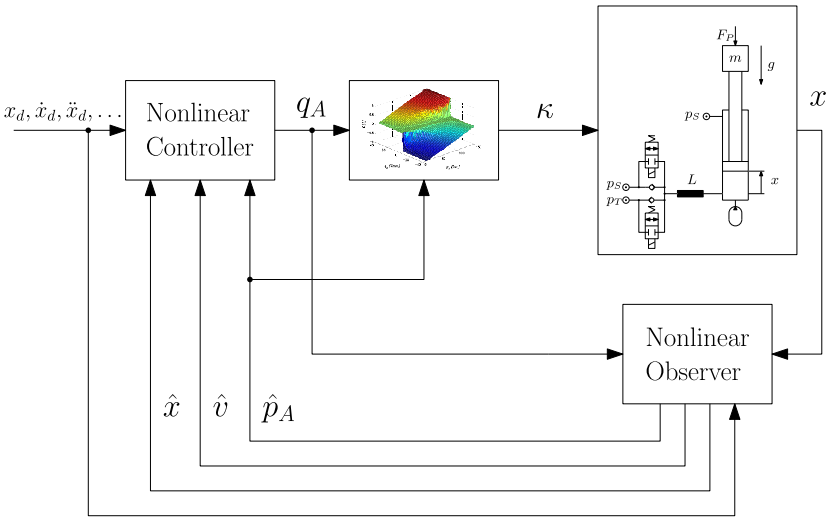

Fig. 11: FBC of a linear hydraulic drive employing a complete observer

In Fig. 14 the closed loop measurements of the flatness based control with a complete observer are illustrated. Now the tracking performance of the HBC is even better than the HPD with a conventional P-controller, while the energy consumption of the HBC is approximately the half of the HPD. In Fig. 15 the measurements for a sinusoidal trajectory at a frequency of $0.2\,Hz$ is illustrated. Also in this case the tracking performance of the HBC with the flatness based control is satisfying and the energy consumption of the HBC is nearly half the HPD consumption.

5 Conclusion

Compared to electric switching control, today only relatively low switching frequencies are feasible in hydraulics, mainly because of the limitations of valve response dynamics. In turn, accumulators for pulsation attenuation have quite high hydraulic capacity which gives the system high softness and significant nonlinear behaviour. Simple proportional control of such a converter may lead to bad performance, for instance, if high dry friction is present in the system. The system composed of the buck converter and the linear drive is flat in the sense of control theory, if the converter is modelled as a continuous system. This suggests to employ a flatness based controller. That controller requires all states of the corresponding system model to be known. It could be shown, that in case of a measureable position signal a nonlinear observer can be used. The controller brings a substantial performance gain over a simple proportional controller, but no improvement of efficiency. Its tracking behaviour is as

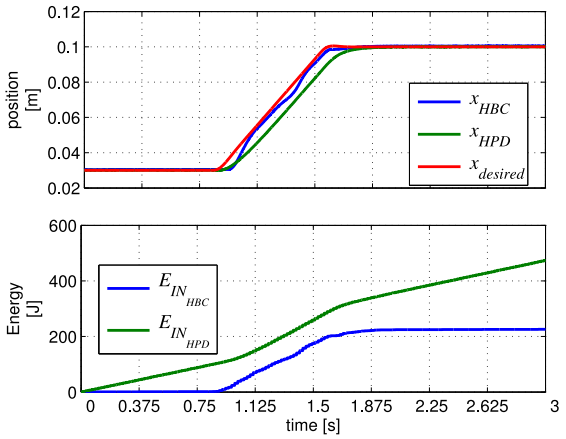

(a) Extending piston movement

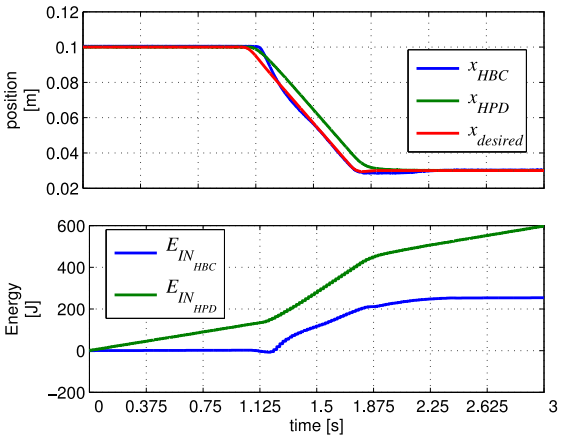

(b) Retracting piston movement

Fig. 14: Measurements of HBC with flatness based control compared with HPD

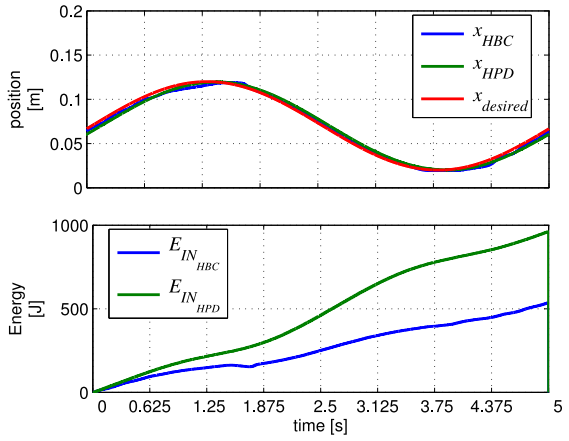

Fig. 15: Measured sinusoidal trajectory of FBC vs. HPD

good as that of a conventional hydraulic servo-drive for the investigated motions, the energy consumption is approximately only one half, at least in the investigated cases. This is a remarkable improvement in view of the relatively low power rating of that converter and the deficiencies of the used check valves. It is obvious that significantly higher switching frequencies require much smaller accumulators. In some cases even fluid compressibility in the cylinder chamber might be enough. Such systems behave much simpler and simple controllers might provide sufficient performance. Future work will focus on improved key components, in particular on better check valves and on prototypal tests of the buck converter for specific industrial applications.

Acknowledgment

This work has been supported by the Austrian COMET-K2 programme of the Linz Center of Mechatronics (LCM), and was funded by the Austrian federal government and the federal state of Upper Austria.

References

[1] J. Linares-Flores, H. Sira-Ramírez, DC motor velocity control through a DC-to-DC power conterter, in: Proceedings of the 43^{rd} IEEE Conference on Decision and Control, vol. 5, 5297–5302, 2004.

[2] F. Antritter, P. Maurer, J. Regner, Flatness based control of a Buck-Converter driven DC Motor, in: Proceedings of the 4^{th} IFAC Symposium on Mechatronic Systems, 2006.

[3] J. Linares-Flores, H. Sira-Ramírez, A Smooth Starter for a DC Machine: A Flatness Based Approach, in: Proceedings of the 1^{st} International Conference on Electrical and Electronics Engineering, 589–594, 2004.

[4] M. Fliess, J. Lévine, P. Martin, P. Rouchon, Flatness and Defect of Nonlinear Systems: Introductory Theory and Examples, International Journal of Control 61 (1995) 1327–1361.

[5] A. Isidori, Nonlinear Control Systems, $3^{rd}Edition, Springer, London, UK$, 1995.

[6] R. Rothfuß, Anwendung der flachheitsbasierten Analyse und Regelung nichtlinearer Mehrgrößensysteme, Tech. Rep., Fortschr.-Ber. VDI Reihe 8 Nr. 664, Düsseldorf: VDI Verlag, Germany, 1997.

[7] R. Rothfuß, J. Rudolph, M. Zeitz, Flachheit: Ein neuer Zugang zur Steuerung und Regelung nichtlinearer Systeme, Automatisierungstechnik 45 (1997) 517–525.

[8] J. Rudolph, Rekursiver Entwurf stabiler Regelkreise durch sukzessive Berücksichtigung von Integratoren und quasi-statische Rückführungen, Automatisierungstechnik 53 (2005) 389–399.

[9] J. Lévine, Analysis and Control of Nonlinear Systems: A Flatness-based Approach, Springer, Berlin, 2009.

[10] P. Rouchon, Flatness based control of oscillators, Plenary Lecture presented at the 75^{th} Annual GAMM Conference, Dresden/Germany, 2004.

[11] H. Sira-Ramírez, S. K. Agrawal, Differentially Flat Systems, Marcel Dekker, New York, 2004.

[12] M. Fliess, J. Rudolph, Local "tracking observers" for flat systems, in: Proceedings of the Symposium on Control, Optimization and Supervision, CESA '96 IMACS Multiconference, Lille, France, 213–217, 1996.

[13] J. von Löwis, J. Rudolph, Real-time trajectory generation for flat systems with constraints, in: A. Zinober, D. Owens (Eds.), Nonlinear and Adaptive Control, Springer Verlag Berlin Heidelberg, 385–394, 2003.

[14] A. Wolfram, M. Vogt, Zeitdiskrete Filteralgorithmen zur Erzeugung zeitlicher Ableitungen, at - Automatisierungstechnik 50 (2002) 346 – 353.

Nomenclature

A_1	cross-section area of piston ..... $[m^2]$
A_2	cross-section area of annulus chamber $[m^2]$
d_v	viscous friction ..... $[\frac{Ns}{m}]$
e	error
$\mathbf{e}$	error vector
$\hat{\mathbf{e}}$	vector of estimation error
g	gravity ..... $[\frac{m}{s^2}]$
$\mathbf{L}$	observer design matrix
m	dead load ..... $[kg]$
$M_{\mathbf{A}(t)}\mathbf{t}_1^\intercal$	differential operator on the matrix $\mathbf{A}(t)$ and the row vector $\mathbf{t}_1^\intercal$
$N_{\mathbf{A}(t)}\mathbf{b}$	differential operator on the matrix $\mathbf{A}(t)$ and the column vector $\mathbf{b}$
p_{0_G}	gas pre-pressure ..... $[Pa]$
p_A	load pressure ..... $[Pa]$
$\mathbf{Q}$	observability matrix
q_A	flow rate at output of the converter $[\frac{m^3}{s}]$
v	velocity ..... $[\frac{m}{s}]$
V_A	accumulator volume ..... $[m^3]$
x	position ..... $[m]$
x_d	desired position ..... $[m]$
$\hat{\mathbf{x}}$	observer state vector
y_d	desired output
α_i	i^{th} observer parameter
$\Delta\zeta$	deviation of ζ
Δu	deviation between actual and desired set value
$\Delta\mathbf{x}$	deviation between actual and desired state
$\widehat{\Delta\mathbf{x}}$	deviation between estimated and desired state
η	measured quantity
γ_i	i^{th} controller parameter
$\varkappa$	polytropic exponent ..... [1]
$\boldsymbol{\psi}_1$	state transformation
ψ_2	input transformation
$\widetilde{\psi}_2$	state feedback
σ	number of derivatives with respect to time
ς	auxiliary variable
τ_i	i^{th} filter parameter
$\boldsymbol{\Theta}$	state transformation matrix into canonical form
ϑ	auxiliary variable
Υ	auxiliary variable
$\boldsymbol{\zeta}$	state vector in canonical form
$\star$	canonical form